Prediction Method for Transmission Line Fault Probability under Ice Disasters by Modified BPNN

Dexin Li
Power System Technology Center
State Grid JiLin Electric Power Research Institute
Jilin, China
lidexin0323@163.com

Jun Leng
Power System Technology Center
State Grid JiLin Electric Power Research Institute
Jilin, China
874945675@qq.com

Wenqi Han
Power System Technology Center
State Grid JiLin Electric Power Research Institute
Jilin, China
1272662947@qq.com

Song Gao
Power System Technology Center
State Grid JiLin Electric Power Research Institute
Jilin, China
418150396@qq.com

Geng-Chen Li*
Department of Electrical Engineering
Northeast Electric Power University
Jilin, China
605544372@qq.com

Linbo Fu
Department of Electrical Engineering
Northeast Electric Power University
Jilin, China
fulinbo123@aliyun.com

2023 IEEE 7th Conference on Energy Internet and Energy System Integration (EI2) | 979-8-3503-4509-4/23/$31.00 ©2023 IEEE | DOI: 10.1109/EI259745.2023.10512938

***Abstract*—As a vital component of the power system, the safe and reliable operation of the transmission system is a crucial guarantee for stable electricity delivery. As the frequency of extreme weather conditions increases gradually, the secure operation of the transmission system faces significant challenges. Enhancing the resilience of the power system during extreme natural disasters has become a hot research topic. This paper focuses on studying the impact of ice disasters on transmission lines and presents a method for predicting the fault probability of transmission lines, namely the HFAPSO-BPNN prediction model. This method offers faster computation speed compared to traditional model-driven fault rate calculation methods and plays a pivotal role in addressing the resilience of the power system. Finally, through two sets of simulation experiments, the paper confirms the advantages of the proposed method in terms of predictive accuracy and speed.**

***Index Terms*—BPNN, ice disasters, prediction, resilience, transmission system**

I. Introduction

The impact of natural disasters on the electrical power systems has long been a matter of significant concern. Ice disasters are a type of high-impact, low-probability disaster event, prone to causing extensive power disruptions when they occur [1]. For instance, in 2021, a highly severe ice disaster took place in the northeastern region of China. This disaster resulted in the cumulative shutdown of over 400 power lines with a voltage of 10 kV or higher in Jilin Province, causing damage to over 180 power lines with the same voltage level in Liaoning Province. Furthermore, it impacted the electricity supply for more than 170,000 households. The increasing dependence on electricity in modern society highlights the critical importance of the reliability and stability of the electrical power systems for the normal functioning of society and the economy. The probability of transmission line failures, serving as a resilience indicator to assess the system's ability to withstand disasters and severe faults, plays a crucial role [2]–[4]. Predicting the failure probability of transmission lines before disasters occur and implementing corresponding enhancement measures can reduce the losses caused by extreme disasters to the system.

Traditional calculation methods are mainly model-driven. Jones establishes an ice accretion model to estimate the amount of ice accretion on circular objects, which can be used to calculate the impact of ice disasters on power lines [5]. Brostrom takes factors such as wind speed, rainfall rate, and ice thickness into account to build an ice disaster model [6]. While these methods can accurately calculate the results, they suffer from slow computation speeds. The sluggish computational speed means that even if disaster data are predicted in advance, it may not be possible to take appropriate response measures. Therefore, there is a need to develop an efficient method for calculating the fault probability of transmission lines.

With the development of artificial intelligence, numerous machine learning algorithms have been applied across various domains, including the Backpropagation Neural Network (BPNN) [7], [8]. BPNN does not require complex design or coding but rather involves data processing and analysis. By training on historical datasets, it can establish the mapping relationship between inputs and outputs, resulting in a predictive model that achieves data-driven efficiency. As a result, this method has found wide application in the field of power system research. Zhang presented a method based on the Levenberg-Marquardt Backpropagation Neural

This work was supported by the State Grid Jilin Province Electric Power Co., Ltd – Research and Application of Power Grid Resilience Assessment and Coordinated Emergency Technology of Supply and Network for the Development of New Power System in Alpine Region (Project Number is B32342210001).

Network (LM-BPNN) and derived a power routing lifespan extension approach for DC-DC boost conversion systems [9]. In order to achieve high-precision power system load forecasting, introduced an optimization model based on Particle Swarm Algorithm (PSO) [10]. In comparison to traditional model-driven calculation methods, this kind of method exhibits efficient computation speed. However, the algorithm itself has limitations such as a susceptibility to falling into local minima, resulting in lower predictive accuracy. To address these issues, this paper introduces a ice disaster-induced transmission line fault probability prediction method based on Hybrid Firefly Algorithm and Particle Swarm Algorithm (HFAPSO)-BPNN. First, by analyzing the characteristics of traditional Firefly Algorithm (FA) [11] and PSO [12], HFAPSO is proposed. Next, HFAPSO is used to optimize the BPNN model, creating the HFAPSO-BPNN model to overcome the drawbacks of traditional models. Finally, HFAPSO-BPNN is integrated into the research of transmission line fault probability under ice disasters. The accuracy and speed of this method are validated through two comparative experiments.

II. Prediction Model for Transmission Line Fault Probability under Ice Disasters

A. Transmission Line Fault Probability Model under Ice Disasters

The primary harm inflicted by ice disasters on the transmission system occurs when freezing rain descends onto the transmission lines, leading to the formation of ice coatings. These ice coatings exceed the load-bearing capacity designed for the lines. The increase in ice thickness and the enlarged wind-exposed surface area of the lines cause mechanical failures, resulting in line breakages and, consequently, economic losses [5].

The model for the growth of ice thickness along a unit length of a transmission line can be expressed as follow.

$$R_{\mathrm{eq}i,t} = \frac{T}{\pi \rho_{\mathrm{I}}} \sqrt{\left(r_{i,t}\rho_{\mathrm{w}}\right)^2 + \left(3.6\nu_{i,t}W_{i,t}\right)^2} \tag{1}$$

$$W_{i,t} = 0.067 \times r_{i,t}^{0.846} \tag{2}$$

$$q_{i,t} = \int_0^t R_{\mathrm{eq}i,u} du \tag{3}$$

In the equation, $R_{\mathrm{eq}i,t}$ and $q_{i,t}$ represent the increment and thickness, respectively, of ice covering a unit length of transmission line i at time t. T stands for the duration of freezing rain in hours. $r_{i,t}$, $\nu_{i,t}$ and $W_{i,t}$ denote the freezing rain amount, wind speed, and liquid water content in the air at the location of line i at time t, respectively. ρ_w is the density of water, while ρ_I represents the density of the ice cover.

During ice disasters, transmission lines are primarily subjected to two types of forces: vertical forces caused by ice accumulation on the lines and horizontal forces induced by the wind. When constructing a fault probability model for transmission lines, it is crucial to consider both ice and wind forces simultaneously. Based on the ice accumulation model for transmission lines and the wind speed under ice disaster conditions, the representations for the unit length transmission line's ice load and wind load are as follows.

$$L_{\mathrm{I}i,t} = 9.8 \times 10^{-3} \rho_{\mathrm{I}} \pi (\mathrm{D}_i + q_{i,t}) q_{i,t} \tag{4}$$

$$L_{\mathrm{W}i,t} = \mathrm{CS}_i v_{i,t}^2 (\mathrm{D}_i + 2q_{i,t}) \tag{5}$$

In the equation, $L_{Ii,t}$ and $L_{Wi,t}$ represent the ice load and wind load, respectively, on a unit length of transmission line i at time t. D_i is the diameter of line i, and C is a constant coefficient set to $6.964 * 10^{-3}$. S_i is the span factor for line i. The magnitude of wind load is typically dependent on the wind speed in the vicinity of the transmission line. However, under ice disaster conditions, the wind load considers the variation in ice thickness on the transmission line, causing this load type to accumulate similarly to the ice load.

Considering that the two types of loads acting on the transmission line are applied in different directions, it's necessary to consider load synthesis, which involves the combined effects of ice load and wind load. Therefore, under ice disaster conditions, the ice load and wind load on the transmission line are illustrated in Fig. 1.

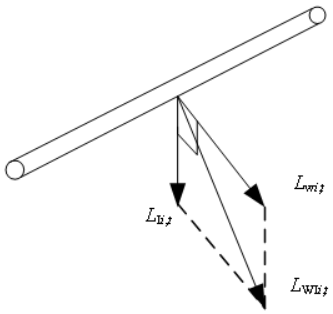

Fig. 1. Illustration of Ice Wind Load on Transmission Lines.

Based on the synthesis of the ice load $L_{Ii,t}$ and the wind load $L_{Wi,t}$ in their respective force directions, the ice-wind load on unit length transmission line i at time t, $L_{Wi,t}$, is determined as follows.

$$L_{\mathrm{WI}i,t} = \sqrt{\left(L_{\mathrm{I}i,t}\right)^2 + \left(L_{\mathrm{W}i,t}\right)^2} \tag{6}$$

When constructing transmission lines, appropriate anti-icing design standards are usually adopted based on the region's characteristics to ensure that the transmission system has a certain level of resistance to ice accumulation. During ice disasters, if the ice thickness exceeds this design standard, it may lead to line breakages. The unit length line fault probability is given as follows.

$$p_f = \begin{cases} 0 & L_{\mathrm{WI}i,t} \le a_{\mathrm{WI}} \\ e^{\left[\frac{0.6931\left(L_{\mathrm{WI}i,t}-a_{\mathrm{WI}}\right)}{b_{\mathrm{WI}}-a_{\mathrm{WI}}}\right]}-1 & a_{\mathrm{WI}} < L_{\mathrm{WI}i,t} < b_{\mathrm{WI}} \\ 1 & L_{\mathrm{WI}i,t} \ge b_{\mathrm{WI}} \end{cases} \tag{7}$$

In the equation, a_{WI} and b_{WI} represent the first and second threshold values for the ice-wind load, respectively. According to the definition of a series network, based on the unit length line fault probability, the fault probability of line i with a length of l at time t can be calculated as follows.

$$p_{i,t} = 1 - (1 - p_f)^l \tag{8}$$

B. Hybrid Firefly Algorithm and Particle Swarm Algorithm

Establish the mathematical model for the traditional FA as follows:

- Set the parameters for FA, which primarily include the maximum attractiveness of firefly individuals β_0, light absorption coefficient γ, and the maximum number of algorithm iterations, among others.
- Initialize the population of fireflies and calculate the relative luminance of each individual firefly based on the formula for relative luminance.
  Each firefly generates its own luminance I, which affects the attractiveness β of the firefly. According to the design rules of FA, the luminance generated by each firefly individual i is related to its objective function value. Therefore, when searching for solutions to an optimization problem, the luminance of a firefly individual can be simply considered proportional to the objective function. Additionally, the luminance of a firefly individual is also influenced by the distance between itself and the target individual. Hence, when the distance between firefly i and j is denoted as r_{ij}, their relative luminance I_{ij} can be expressed as follows.
  $$I_{ij} = I_0 \cdot e^{-\gamma r_{ij}} \tag{9}$$
  In the equation, I_0 represents the maximum luminance of the firefly individual, and r_{ij} represents the spatial distance between firefly i and j. In FA, since the relative luminance of a firefly individual is typically directly proportional to its fitness function value, the relative luminance of an individual is often substituted with its fitness function value in practice.
- Based on the comparison of the fitness function values of firefly individuals, the movement direction of each firefly is determined. When firefly j has a higher relative luminance compared to firefly i, individual i will move toward j.
- Calculate the attractiveness of the firefly individuals. Assuming that, under the condition of a spatial distance r between fireflies i and j, the formula for their attractiveness is as follows.
  $$\beta = \beta_0 \cdot e^{-\gamma r_{ij}} \tag{10}$$
- Calculate the new position of the firefly individuals after their movement and update their positions. After determining the movement direction of the firefly individuals and calculating their attractiveness, the formula for the new position of individual i after its movement is as follows.
  $$x_i(t+1) = x_i(t) + \beta\left(x_j(t) - x_i(t)\right) + \alpha \tag{11}$$
  In the equation, t represents the current iteration count, $x_i(t)$ and $x_j(t)$ stand for the spatial positions of firefly individuals i and j at their current locations, $x_i(t+1)$ denotes the spatial position of firefly individual i after displacement, and α represents the step size factor.
- Increment the iteration count by 1, check whether the termination condition is met, and if it's not met, proceed to the next iteration. Otherwise, output the optimization result.

Establish the mathematical model for the traditional PSO as follows.

- Configure the parameters for PSO, primarily including the number of particles in the population (pop), particle dimension (D), the number of iterations ($iter_{\max}$), inertia weight (ω), and learning factors (c_1 and c_2).
- Randomly initialize the population to obtain the position of each particle (X_i) and its velocity (V_i), and calculate the fitness function value ($f(X_i)$) for each particle.
- Determine the individual best solution (p_{best}) and the global best solution (g_{best}).
- Update the individual positions and velocities based on Eq.(12) and Eq.(13).
  $$v_i = \omega v_i + c_1 r_1\left(p_{best} - x_i\right) + c_2 r_2\left(g_{best} - x_i\right) \tag{12}$$
  $$x_i = x_i + v_i \tag{13}$$
  In the equations, ω represents the weight, indicating the degree to which the particle's current behavior is influenced by its past motion state. c_1 and c_2 are learning factors, reflecting the proportion of learning from "self-experience" and "social experience". r_1 and r_2 are random numbers within the range [0,1].
- Update p_{best} and g_{best} based on the fitness function values of each particle.
- Increment the iteration count by 1, check whether the termination condition is met, and if it's not met, proceed to the next iteration. Otherwise, output the optimization result.

Through the analysis of FA and PSO, it is observed that FA can escape local optima by diversifying the population, while PSO is better at converging towards global optima. Therefore, by combining these two algorithms and leveraging their respective strengths, HFAPSO is developed, ultimately enhancing the optimization performance of the algorithm.

The specific workflow and mathematical model for HFAPSO are as follows.

- Initialize the parameters for FA and PSO.
- Randomly generate the initial population and calculate p_{best} and g_{best}.
- Calculate the relative luminance (I_{ij}) between particle i and j.
- Calculate the distances between particle i and p_{best}, as well as between particle i and g_{best}, based on Eq.(14) and Eq.(15).

$$r_{pi} = \sqrt{\sum_{k=1}^{pop} \left(p_{best_i} - x_i\right)^2} \tag{14}$$

$$r_{gi} = \sqrt{\sum_{k=1}^{pop} \left(g_{best_i} - x_i\right)^2} \tag{15}$$

- Determine the attraction relationship between particle i and j. For particles with higher relative luminance, apply random perturbation based on Eq.(16). For particles with lower relative luminance, update their positions using Eq.(17).

$$x_i\left(t+1\right) = x_i\left(t\right) + \alpha \tag{16}$$

$$\begin{aligned} x_i\left(t+1\right) = x_i\left(t\right) + \beta_0 \cdot e^{-\gamma r_{pi}^2}\left(p_{best_i} - x_i\left(t\right)\right) \\ + \beta_0 \cdot e^{-\gamma r_{gi}^2}\left(g_{best_i} - x_i\left(t\right)\right) + \alpha \end{aligned} \tag{17}$$

- Calculate the current p_{best} and g_{best} based on the positions of the particles after movement.
- Increment the iteration count by 1, check whether the termination condition is met, and if it's not met, proceed to the next iteration. Otherwise, output the optimization result.

C. Fault Probability Prediction Model for Transmission Lines Based on HFAPSO-BPNN

The traditional BPNN is an artificial neural network model introduced in 1986. It effectively addresses the issue of updating connection weights within the neural network. BPNN consists of three main components: the input layer, the hidden layer, and the output layer, as depicted in Fig. 2.

The number of nodes in the input and output layers is determined by the dimensions of the input and output data in the dataset. However, the number of nodes in the hidden layer is calculated using an empirical equation. The specific empirical equation is as follows.

$$k = \sqrt{n_{in} + n_{out}} + r \tag{18}$$

In the equations, n_{in} and n_{out} represent the number of nodes in the input and output layers, and r represents a random integer from [1,9].

Traditional BPNN heavily relies on the proper setting of initial weights and thresholds. Inadequate settings can lead to BPNN easily getting stuck in local minima, resulting in low prediction accuracy. Therefore, this paper introduces HFAPSO as an optimization approach to determine the optimal initial values for weights and thresholds of traditional BPNN. Using a dataset that includes different ice storm quantities, wind speeds, ice storm durations, and transmission line fault probabilities during such disasters, the model is trained. The dataset is partitioned into training and testing sets in a specific proportion. Through continuous training of the model, a fault probability prediction model for transmission lines based on HFAPSO-BPNN is developed. The specific flowchart of the fault probability prediction model for transmission lines based on HFAPSO-BPNN is illustrated in Fig. 3.

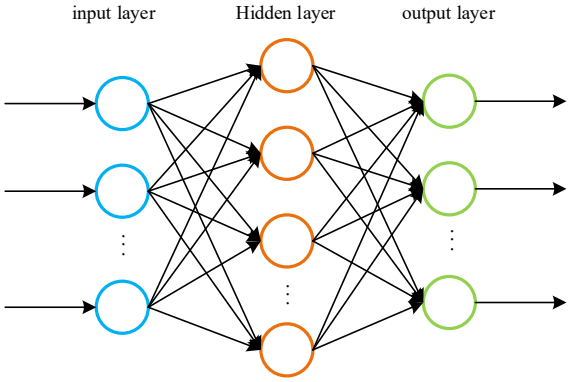

Fig. 2. The schematic diagram of traditional BPNN.

The algorithm stops running when the maximum number of iterations is reached or when the desired prediction accuracy is achieved. At this point, the final prediction results are generated.

III. Experimental Results and Discussion

In this article, we conduct simulation analysis and validation using the IEEE RTS 79 system as an example. The topological diagram of the IEEE RTS 79 system is shown in Fig. 4.

The IEEE RTS 79 system consists of 24 nodes, 38 transmission lines, and a maximum load of 2850 MW. It is assumed that all nodes and transmission lines in the system are exposed to an outdoor environment susceptible to icing. A dataset of line failure rates under ice disaster scenarios is generated, comprising 5000 sets of data. This dataset is split into a training set and a test set with a 4:1 ratio for training the BPNN prediction model based on the HFAPSO.The model is compared with traditional BPNN, FA-BPNN, and PSO-BPNN. The specific parameter settings for the simulation experiments are recorded in Tab. I.

All simulation results were obtained using the PyCharm 2019.3.3 platform on a PC equipped with an Intel(R) Core(TM) i9-13900K CPU operating at 3GHz and 32GB of RAM.

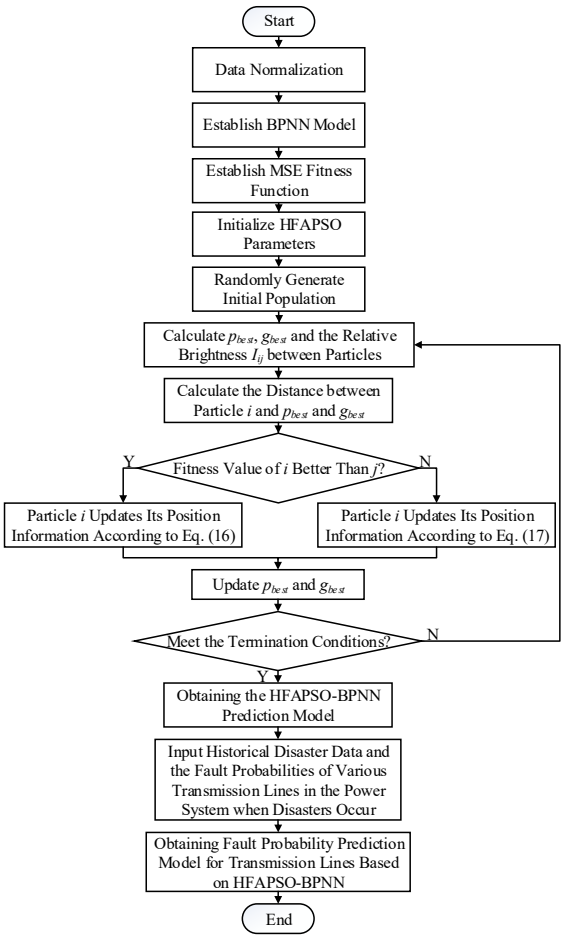

Fig. 3. Flowchart of HFAPSO-BPNN Prediction Method for Transmission Line Fault Probability.

TABLE I
PARAMETER CONFIGURATION

FA	PSO	HFAPSO
$pop = 80$	$pop = 80$	$pop = 80$
$iter_{\max} = 1000$	$iter_{\max} = 1000$	$iter_{\max} = 1000$
$\beta_0 = 1$	$c_1 = c_2 = 2$	$\beta_0 = 1$
$\gamma = 1$	$\omega = 0.9$	$\gamma = 1$

A. Accuracy Analysis

The MSE was used as the criterion to calculate the computational accuracy of each method in the IEEE RTS 79 testing system. The specific comparative experimental results are recorded in Tab. II.

B. Efficiency Analysis

Simulation experiments for the IEEE RTS 79 system were conducted using the traditional model-driven approach to determine the line failure rates. The computation time for the HFAPSO-BPNN prediction results was compared to validate the speed of this approach. A comparison was made using

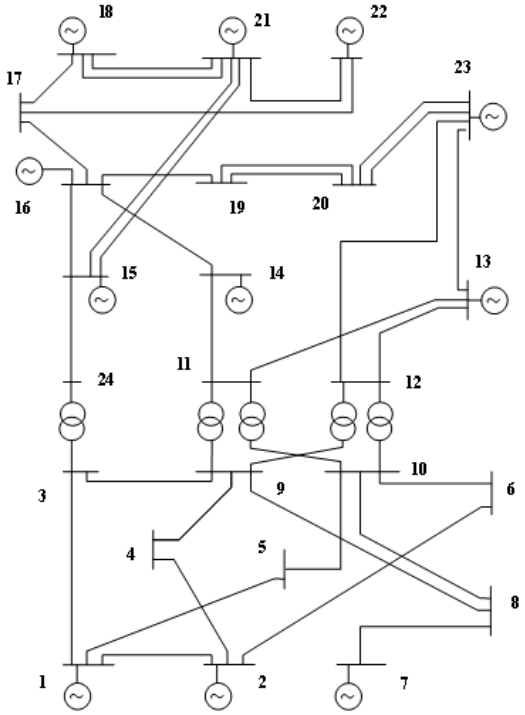

Fig. 4. Topology Diagram of IEEE RTS 79 System.

TABLE II
THE EXPERIMENTAL RESULTS FOR MSE COMPARISON

Algorithm	MSE
BPNN	0.178
FA-BPNN	0.092
PSO-BPNN	0.098
HFAPSO-BPNN	0.062

500 sets of data from the test set, and the results were averaged. Specific comparative experimental results are shown in Tab. III.

TABLE III
THE EXPERIMENTAL RESULTS FOR COMPUTATION TIME COMPARISON

Model-driven	HFAPSO-BPNN
577.61s	0.0106s

The above case results indicate that the method proposed in this paper meets the required accuracy in predictions. Furthermore, compared to the traditional method, the computational efficiency has been improved by 99.981 percent.

IV. CONCLUSION

The impact of extreme natural disasters on the power system cannot be ignored, as severe disasters can lead to widespread power outages and significant property losses. This paper focuses on the study of the impact of ice disasters on transmission lines and proposes a method for predicting the fault probability of transmission lines. This method utilizes HFAPSO to optimize the traditional BPNN, overcoming the

drawbacks of traditional methods that tend to get stuck in local minima. Compared to traditional model-driven fault rate calculation methods, this method offers faster computation speed, making it crucial for addressing the resilience of the power system. Through simulation experiments, this paper compares the predictive accuracy of four BPNN models and conducts simulation experiments to compare the speed of the proposed method against traditional methods, confirming its advantages.

REFERENCES

[1] R. Cloutier, A. Bergeron, and J. Brochu, "On-load network de-icer specification for a large transmission network," *IEEE transactions on power delivery*, vol. 22, no. 3, pp. 1947–1955, 2007.

[2] P. Gasser, P. Lustenberger, M. Cinelli, W. Kim, M. Spada, P. Burgherr, S. Hirschberg, B. Stojadinovic, and T. Y. Sun, "A review on resilience assessment of energy systems," *Sustainable and Resilient Infrastructure*, vol. 6, no. 5, pp. 273–299, 2021.

[3] B. Ti, G. Li, M. Zhou, and J. Wang, "Resilience assessment and improvement for cyber-physical power systems under typhoon disasters," *IEEE Transactions on Smart Grid*, vol. 13, no. 1, pp. 783–794, 2021.

[4] E. B. Watson and A. H. Etemadi, "Modeling electrical grid resilience under hurricane wind conditions with increased solar and wind power generation," *IEEE Transactions on Power Systems*, vol. 35, no. 2, pp. 929–937, 2019.

[5] K. F. Jones, "A simple model for freezing rain ice loads," *Atmospheric research*, vol. 46, no. 1-2, pp. 87–97, 1998.

[6] E. Brostrom, J. Ahlberg, and L. Soder, "Modelling of ice storms and their impact applied to a part of the swedish transmission network," in *2007 IEEE Lausanne Power Tech*. IEEE, 2007, pp. 1593–1598.

[7] D. E. Rumelhart, J. L. McClelland, and C. PDP Research Group, *Parallel distributed processing: Explorations in the microstructure of cognition, Vol. 1: Foundations*. MIT press, 1986.

[8] F. Pan, H. Wen, X. Gao, H. Pu, and Z. Pang, "Clone detection based on bpnn and physical layer reputation for industrial wireless cps," *IEEE Transactions on Industrial Informatics*, vol. PP, no. 99, pp. 1–1, 2020.

[9] J. Zhang, J. Tian, A. M. Alcaide, J. I. Leon, S. Vazquez, L. G. Franquelo, H. Luo, and S. Yin, "Lifetime extension approach based on levenberg-marquardt neural network and power routing of dc-dc converters," *IEEE Transactions on Power Electronics*, 2023.

[10] Y. Yao, J. Lv, W. Gu, J. Zhao, and Y. Liu, "Short term power load forecasting method based on particle swarm optimization algorithm and recurrent neural network," in *2022 IEEE 4th International Conference on Civil Aviation Safety and Information Technology (ICCASIT)*. IEEE, 2022, pp. 814–817.

[11] X.-S. Yang, "Firefly algorithm, stochastic test functions and design optimisation," *International journal of bio-inspired computation*, vol. 2, no. 2, pp. 78–84, 2010.

[12] J. Kennedy and R. Eberhart, "Particle swarm optimization," in *Proceedings of ICNN'95-international conference on neural networks*, vol. 4. IEEE, 1995, pp. 1942–1948.